Slag-Metal Reactions in the Electroslag Process

Slag-metal reactions are fundamentally controlled by the thermodynamic driving force, the physical nature of the reaction products, and mass transport in the liquid slag and metal phases

BY B. M. PATCHETT AND D. R. MILNER

ABSTRACT. Slag-metal reactions in electroslag melting have been evaluated in terms of the fundamental controlling parameters. Simple metal systems using pure aluminum and iron, and binary iron alloys, have been melted in inert fluxes to which known quantities of reactive constituent were added. Ingots, fluxes, slags and electrode tips were analyzed chemically and metallographically, and slag bath temperatures were measured with sheathed thermocouples. Aluminum was also melted in transparent silica crucibles, and motion picture films of the melting process provided information on the velocity of the slag motion and its influence on metal transfer and droplet size. Bath velocities of about 100 cm/sec circulate the slag past the electrode tip and detach some of the molten metal as showers of small droplets.

Most of the reaction occurs at the electrode tip. This is due to the high surface area-to-volume ratio of the melting metal and the intense stirring in the reacting slag and metal phases. The fluid motion is caused by the action of the Lorentz forces and rapidly transfers the reactive constituents towards the reaction zone at the slag-metal interface. At the interface there are boundary layers in the flux and the metal, and it is diffusion across these boundary layers that controls the rate of reaction. The thermodynamics of the reaction determines the equilibrium state established at the interface and hence the concentration, or activity, gradient causing diffusion across the boundary layer.

A highly favorable reaction produces a high concentration gradient and hence a high rate of reaction. The nature of the reaction product also influences the rate of reaction. Liquid miscible reaction products readily diffuse and are transported away. Gaseous reaction products formed at the interface slow the rate of reaction by interfering with the diffusion of reactants through the slag boundary layer, and solid reaction products slow the reaction rate by blocking off part of the area available for reaction. The rate of reaction is particularly high where the reactant in the slag is soluble in the metal and is transported into, and reacts with elements in, the bulk of the metal, e.g., the oxidation of silicon and carbon in steel by iron oxide in the slag.

B. M. PATCHETT is with the Department of Materials, Cranfield Institute of Technology, Cranfield, Bedfordshire, England, and D. R. MILNER is with the Department of Industrial Metallurgy, The University, Birmingham, England. *Paper presented at the AWS 53rd Annual Meeting held in Detroit, during April 10-14, 1972.*

Introduction

Slag-metal reactions are of importance in many fusion welding processes, but comparatively little is known about the mechanisms which control them. The predominant reason for this is that slag-metal reactions have been associated primarily with the arc welding of ferrous materials, and they are therefore only a part of the difficult problem of developing practically effective fluxes and electrode coatings.

Over a period of 70 years of largely empirical development, fluxes have been devised to satisfy a multiplicity of requirements such as arc stability, protection of the weld metal from the atmosphere, weld metal deoxidation and alloying, ease of slag removal, etc. With present highly evolved industrial fluxes this results in many chemical reactions occurring simultaneously under the complex physical conditions created by the electric arc, so that the fundamental analysis of the reactions taking place is very difficult. The usual approach is to assume that a state of thermodynamic equilibrium is attained, on the basis that the high temperatures and high surface-to-volume ratio counteract the short time available for reactions to be completed.[1] The chemical compositions of the reaction products in the metal and slag phase are then analyzed in terms of thermodynamic data extrapolated from steel-making and an "effective reaction temperature" is arrived at.

The temperatures so calculated for covered electrode and submerged arc welding vary between 1500 and 2100 C.[2-6] This variation in effective reaction temperature, together with the fact that different elements in the same weld, e.g., silicon and phosphorus, react as though their effective reaction temperatures differed,[5] plus the further fact that slag and metal compositions depend on welding speed,[6] rate and size of droplet transfer[7] and mass transfer,[8] all suggest that equilibrium is not attained. The concept of an "effective reaction temperature" is thus an approximation to an otherwise difficult to evaluate situation, in which reactions are attempting to attain to an equilibrium corresponding to some higher temperature and kinetic processes determine the extent to which they occur.

By contrast the electroslag process offers the possibility of the use of much simpler fluxes under conditions in which slag-metal reactions can be more readily evaluated, since it utilizes resistance heating in the slag and does not involve problems of arc stability and the other complexities of arc welding encountered when using simple slags.[9] Most work on slag-metal reactions in the electroslag process has been related to the use of the technique for the refining of high quality steels where some evaluation has been made of the reactions giving rise to contamination and inclusions.[10] Loss of essential elements and the presence of inclusions is related to the use of oxides in the flux, and it has been found that the order of reactivity of various oxides is that which would be predicted from their thermodynamic stability.[10]

The processes which determine the extent to which reactions take place have been investigated for a model system using low melting point organic and inorganic materials by Crimes.[11] In these experiments the reaction between droplets and the fluid through which they fall has been examined. It was found that the reaction is controlled by diffusion through a boundary layer at the reacting interface, with the rate controlling step in the boundary layer of either the simulated metal or the slag phase, depending on the circumstances. The bulk of reaction occurred during droplet transfer rather than during droplet formation or at the "ingot". Such a model, however, omits the electromagnetic forces which arise from current flow and which are liable to be of considerable significance. (In arc welding such forces have been shown to exert a very marked effect on mass transport and therefore on the extent of reaction.[12]) In electroslag welding the composition of the fluxes used has been strongly influenced by covered electrode and submerged arc experience, although it has also been realized that with less complex conditions simpler principles of flux design are possible.[13]

The objective of the present work has been to clarify the reaction processes in electroslag welding by approaching the problem in three stages. First, the physical conditions of melting, fragmentation and transfer of electrode material, slag motion and temperature are considered. In the second stage simple (non-industrial) systems involving massive reactions have been analyzed to determine the major controlling parameters. Then in the third stage simplified industrially significant reactions are evaluated in terms of the principles established in the first two stages.

Table 1 — Chemical Composition of Slags and Ingots Melted in Inert Fluxes

Base metal	Inert flux	Slag composition, % Al	Electrode composition % Na	% K	Ingot Composition % Na		% K
Al	20% NaF-KCl	0.70	< .001	< .001	.055		.002
		% Fe	% C	% Si	% C	% Si	% Ba
Fe	MgF_2	1.08	.02	< .01	.02	< .01	—
Fe	BaF_2	1.07	.02	< .01	.02	< .01	—
Fe-C	BaF_2	1.10	.20	< .01	.19	< .01	.001
Fe-Si	MgF_2	—	—	0.91	—	0.85	—
Fe-Si	BaF_2	1.00	—	0.91	—	0.84	—

Experimental

In typical industrial systems involving multi-component metals and fluxes several competing reactions are usually taking place simultaneously. These bring about small but significant changes in the composition of the deposited metal, but the fact that only limited changes occur makes chemical, metallographic and theoretical analyses difficult. Thus for this research simple systems have been selected involving the minimum of constituents in the flux and metal, while the first reactions considered have involved massive and therefore readily detectable changes in composition.

Two metal systems, based on aluminum and iron, have been examined by melting in an inert flux to which a reactive constituent has been added. With the lower melting point aluminum system it was possible to observe the metal transfer and slag motion by melting in transparent silica crucibles. A massive reaction with iron was examined by putting nickel oxide in the flux to give transfer of nickel into the iron. With aluminum two reactions involving massive transfer of an alloying element from the slag to the metal were investigated by putting copper chloride or copper oxide in the flux as the active constituent. In all three systems the element freed from the slag is completely miscible in the metal and forms readily analyzed alloys.

The industrial type reactions investigated were based on iron and steel. They were of two types: first, reactions involving transfer of silicon or manganese into the molten metal from SiO_2 or MnO_2 containing slags; second, the removal of silicon and carbon from electrode wires by slags containing various oxides.

The inert fluxes were chosen on the basis of three criteria: suitable

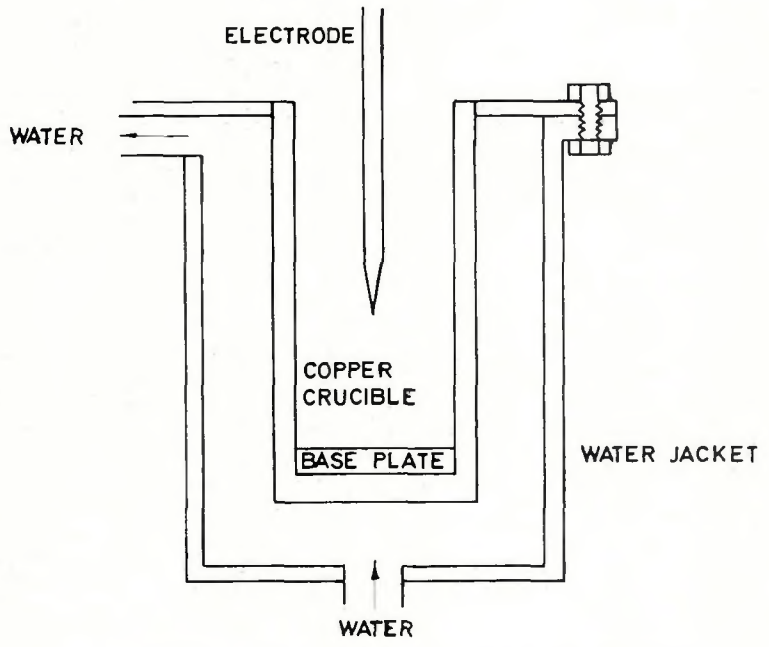

Fig. 1 — Diagram of the electroslag apparatus for ingot deposition

Table 2 — Chemical Composition of Experimental Electrodes, %

Constituent	Al	Fe	Fe-C	Fe-C	Fe-Si
C	—	0.02	0.12	0.19	0.01
Mg	0.025	—	—	—	—
Cu	0.05	—	—	—	—
Zn	0.01	—	—	—	—
Si	0.10	<.01	<.01	<.01	<.91
Na	<.001	—	—	—	—
K	<.001	—	—	—	—
Other		<.01	<.01	<.01	<.01

melting and boiling points, high thermodynamic stability, and lack of solubility of any of the constituents in the liquid or solid metals. On this basis the 20 wt% NaF-KCl eutectic was chosen for aluminum. For the iron and iron alloys two alkaline earth fluorides — MgF_2 and BaF_2 — were used; these have the maximum difference in density of the suitable fluorides and therefore enabled this variable to be examined. Analysis of ingots deposited from the various electrode materials using these fluxes showed only a slight rise in the sodium level in the aluminum ingots, from <0.001 wt% to 0.055 wt%, and a drop in silicon content of the iron-silicon alloy from 0.91 wt% to 0.85 wt% — Table 1.

The experimental electroslag ingots were cast by initiating melting under a layer of granulated flux with a high frequency spark between the pointed electrode tip and a base metal of electrode composition. A water-cooled copper crucible of 28 mm diam by 75 mm depth was used for the bulk of the experimental work — Fig. 1. A transparent silica crucible of similar dimensions was used to observe and photograph the electroslag deposition process with aluminum electrodes.

The molten slag and metal were protected from the atmosphere by a flow of argon until solidification had finished. Deposition conditions were standardized as far as possible for each metal to facilitate comparisons among the different reactive systems. The aluminum electrode feed rate was 184 m/hr (121 ipm), giving a melting condition of 50-60v at 100–150 amp, and the iron electrode feed rate was 114 m/hr (92 ipm), with a potential of 50–60 v and a current of 400-450 amp. Flux composition had some effect on these values as did, of course, experiments in which the influence of melting rate was examined. Any deviations are given in the text. Direct current with electrode positive polarity was used for all experiments.

The electrodes were 3.2 mm diam by 2 m long; the chemical compositions of the various alloys used are given in Table 2. Fluxes were mixed from laboratory-grade chemicals and sintered in the solid state before crushing and sieving, to yield granular material with a particle size between + 300 μ and −2800 μ (+52 mesh to −6 mesh). Slag bath temperatures were measured with sheathed thermocouples; platinum-platinum/rhodium couples were used for aluminum and tungsten-tungsten/rhenium for iron. Metallographic and chemical analyses of the fluxes, slags, ingots and electrode tips were used to trace the progression of mass transfer between the slag and the metal phases.

Physical Conditions During Ingot Deposition

The crucible was filled with granulated flux before starting deposition of an ingot, and more flux was added as melting took place to keep the crucible nearly full. The solidified slag yield was 25–30 cc for each ingot cast. Deposition occupied 30–45 sec per ingot depending on the electrode feed rate used. To assess the extent to which solidification occurred during deposition, iron rods were plunged into several aluminum ingots at the instant when the melting current was switched off. The rods penetrated within 5mm of the bottom of the ingots showing that virtually the whole ingot was molten until the end of deposition. Tungsten rods plunged into iron ingots gave the same result.

Temperatures in the slag baths were recorded by thermocouples immersed between the electrode and the crucible wall. Slag temperatures were 1000 ± 50 C during aluminum deposition and 1900 ± 100 C during iron deposition. Moving the thermocouples around in the slags did not give rise to any observable changes in temperature, showing that the slag bath temperature was essentially uniform.

Slag Motion and Metal Transfer. Aluminum was melted into the inert NaF-KCl flux and also the same flux with a highly reactive addition of 25 wt% $CuCl_2$. Although the inert slag was water-clear when melted on its own, it quickly became opaque when aluminum was melted into it. To obtain a visual record of the melting process it was therefore necessary to limit the depth of slag between the crucible wall and the electrode tip by off-setting the electrode to the camera side of the crucible after melting conditions were established. Color motion picture films at 18 and 400 frames/sec showed that the slag bath flowed downwards past the electrode tip at 50–100 cm/sec in the inert slag, and then upward at the crucible walls giving a continuous circulation of the slag bath as in

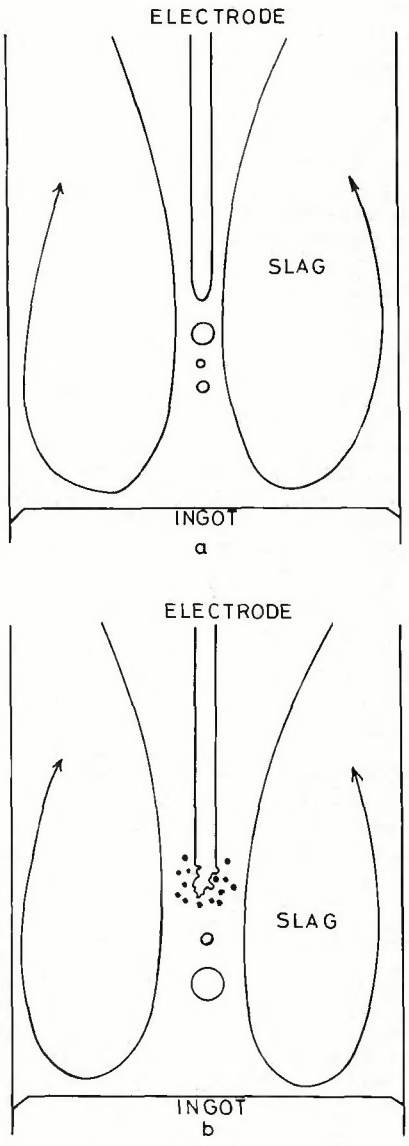

Fig. 2 — Diagram of slag motion and metal transfer observed with the melting of aluminum, (a) with an inert flux, showing form of slag motion, (b) with a reactive flux giving rise to a gaseous reaction product and submerged arcing and irregular droplet transfer

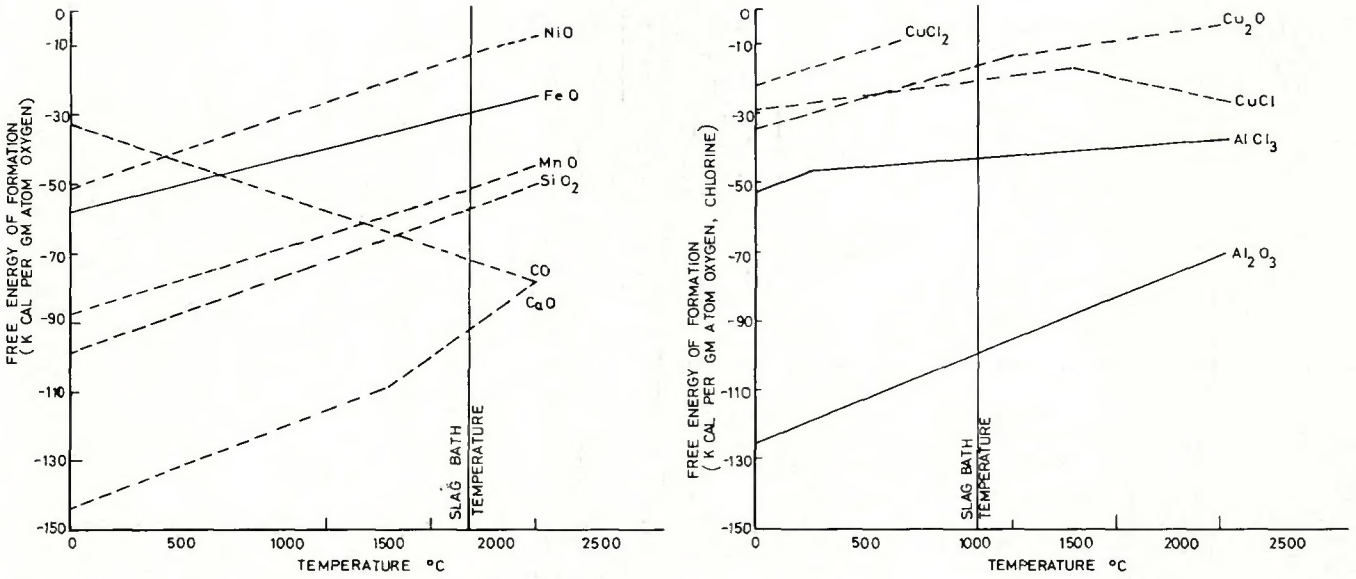

Fig. 3 — Left, the free energy of formation of iron compounds and associated reactive slag compounds and reaction products; right, the free energy of formation of aluminum compounds and associated reactive slag compounds

Fig. 2a. Occasional submerged arcing was observed in the slag at the electrode tip. The visible metal transfer took place as intermittent showers of small droplets with a group velocity of 50–75 cm/sec.

In the reactive slag the flow pattern followed the same general trend, but there was much more submerged arcing and a great deal of random activity at the electrode tip and disturbance of metal transfer — Fig. 2b. This was probably associated with evolution of aluminum chloride gas at the electrode tip as a result of the reaction:

$$(CuCl_2) + Al \leftrightarrows \underline{\%\ Cu} + [AlCl_3]$$

The solidified slags from these experiments and also slags from the deposition of iron ingots contained approximately 1 wt% of metallic droplets (see Figs. 6, 10 and 13).

Systems Showing Massive Reaction

It was found that the rate of reaction varied considerably for the three systems examined. This was attributed to the fact that three types of reaction product were formed — liquid, gaseous and solid, with the rate of reaction decreasing in this order. The reactions are therefore considered individually in these terms. (The reaction products and their state at operating temperatures for the systems considered in this paper are given in Table 3.)

Liquid Reaction Product. Pure iron electrodes were melted in fluxes containing NiO additions to the BaF_2 and MgF_2 inert carriers. The reaction involved is:

$$(NiO) + Fe \leftarrow\rightarrow \underline{\%\ Ni} + (FeO)$$

The reaction will proceed strongly to the right at 1900 C since nickel oxide is much less stable than iron oxide — Fig. 3a. There was a very large transfer of nickel from the slag to the metal, with virtually all of the nickel removed from the slag (Table 4) so that the ingot composition was a linear function of the vol % NiO in the flux — Fig. 4. There was less transfer with the MgF_2 based fluxes which, having a lower density, did not contain as much nickel per unit volume as the BaF_2 based fluxes. Ingot compositions were substantially uniform from top to bottom — Table 4.

More detailed information on the reaction mechanism came from an analysis of the droplet tips and slags. The droplet shown in Fig. 5a apparently formed under comparatively stable conditions; it was obtained with a flux containing 25 wt% NiO and shows a surface layer rich in nickel with a particularly high nickel concentration at the neck of the drop. Electron probe microanalysis showed that the nickel rich regions at the surface and neck of the drop contained 50 to 65 wt% nickel, while the body of the drop had a comparatively constant nickel content of 15–20 wt%. The droplet in Fig. 5b has been displaced. As a result, the surface layer has broken up and parts of it have been swept in with traces of high nickel content ma-

Table 3 — Physical State of Reaction Products During Electroslag Melting

Electrode metal	Slag bath temperature, C	Reactive slag compound	Reaction product	Melting point, C	Boiling point, C	Physical state during reaction
Al	1050	Oxide	Al_2O_3	2027	>2500	Solid
Al		Chloride	$AlCl_3$	—	180	Gas
Fe	1900	Oxide	FeO	1368	>2500	Liquid
Fe		Fluoride	FeF_2	1102	1827	Gas
Fe		Chloride	$FeCl_2$	677	1026	Gas
Fe-C	1900	Oxide	CO	<25	<25	Gas
Fe-Si	1900	Oxide	SiO_2	1610	2500	Liquid
Fe-Si		Fluoride	SiF_4	<25	<25	Gas

terial showing the pattern of fluid flow; in this case the body of the drop contained 10–15 wt% and the ingot 22–24 wt% nickel.

All of the slags contained metallic droplets and dendrites which were rich in nickel (Fig. 6), while the slag surrounding the droplets was virtually devoid of nickel, but contained large quantities of iron. Thus the residual nickel content of the slags can be largely attributed to small droplets trapped from the metal transfer process, while iron is present in two forms — as metallic iron in the droplets and as iron oxide in the slag, which was not completely miscible in the solid state with the BaF_2 carrier.

An increase in the electrode feed speed by a factor of 2½ was used to assess the effect of a higher melting rate using the 25 wt% NiO-BaF_2 flux. The new deposition conditions were: 284 m/hr (186 ipm) electrode feed speed 30–35 v, 650 amp. At the higher melting rate virtually all of the available nickel was still transferred to the ingot as before (Table 5) although the nickel content of the ingot was lower, since a smaller proportion of the flux above the ingot melted than for the standard deposition conditions.

Gaseous Reaction Product. A high driving force giving massive reaction, but with a gaseous reaction product, was involved when melting pure aluminum with fluxes containing cupric chloride. The reaction is of the form:

$$3(CuCl_2) + 2Al \rightleftarrows 3\ \text{wt\%}\ \underline{Cu} + 2[AlCl_3]$$

As shown by Fig. 3b, this reaction will proceed strongly to the right. At the standard electrode feed speed of 183 m/hr (120 ipm) for aluminum, the operating voltage was 65 v and the current about 100 amp. Considerable fuming and some submerged arcing occurred during deposition, especially in slags containing large amounts of $CuCl_2$. The amount of copper transferred to the ingots was again a linear function of the flux

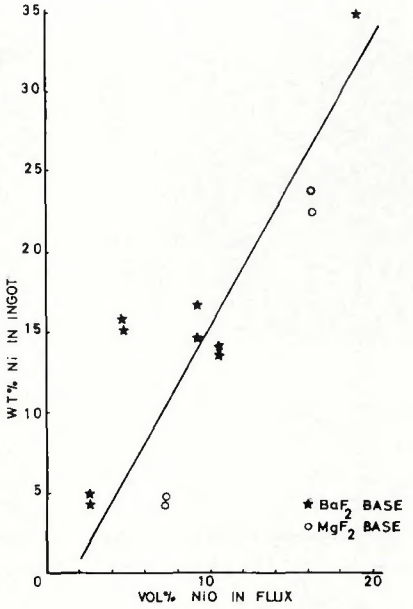

Fig. 4 — Ingot composition vs. flux composition for pure iron melted in NiO-bearing slags

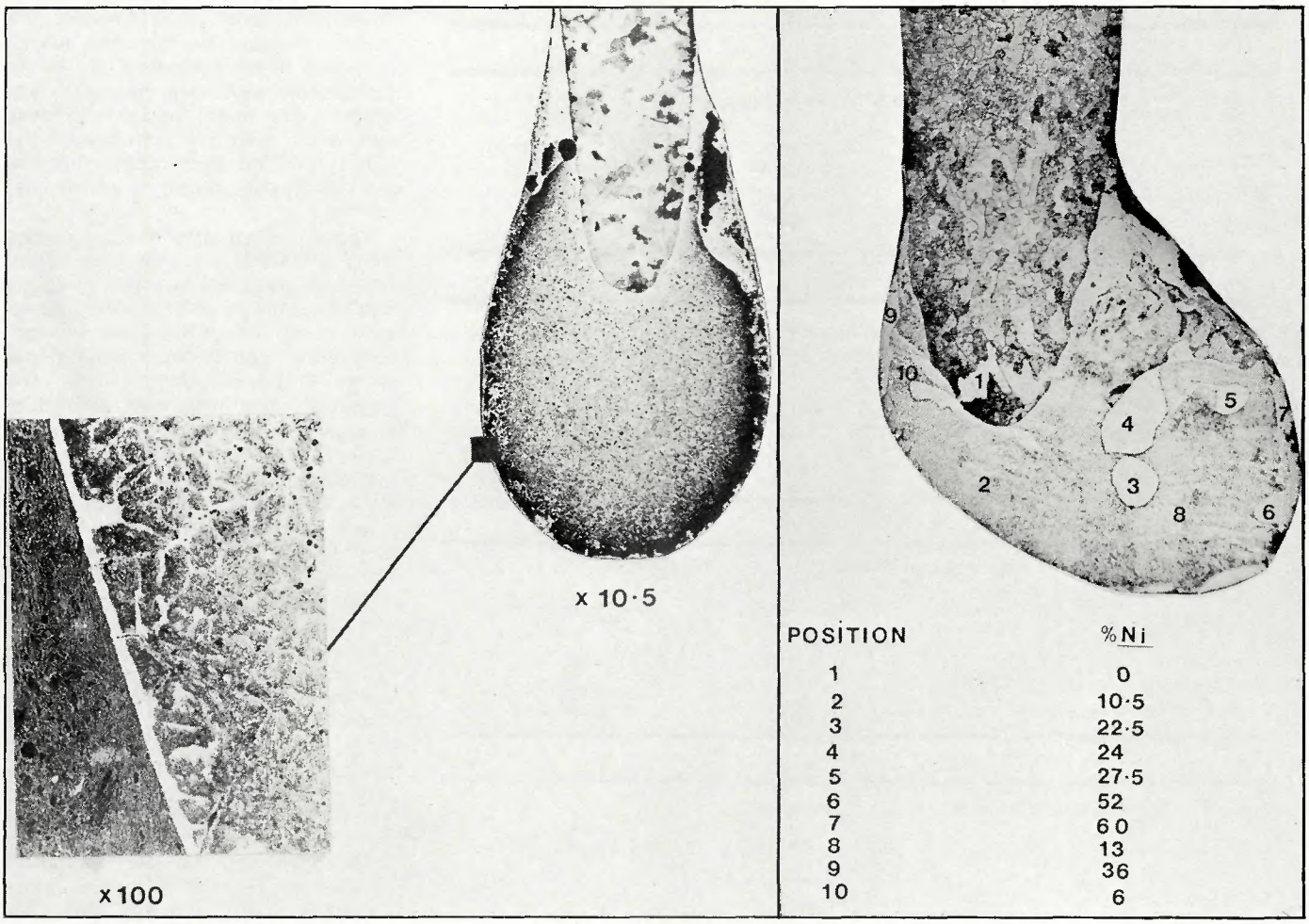

Fig. 5 — The pattern of Ni absorption by pure Fe at the electrode tip obtained with a flux containing 25 wt% NiO: left, showing the high concentration of Ni at the metal surface and at the neck of the droplet; right, showing the macroscopic mixing of alloyed surface layers by stirring forces in the molten metal

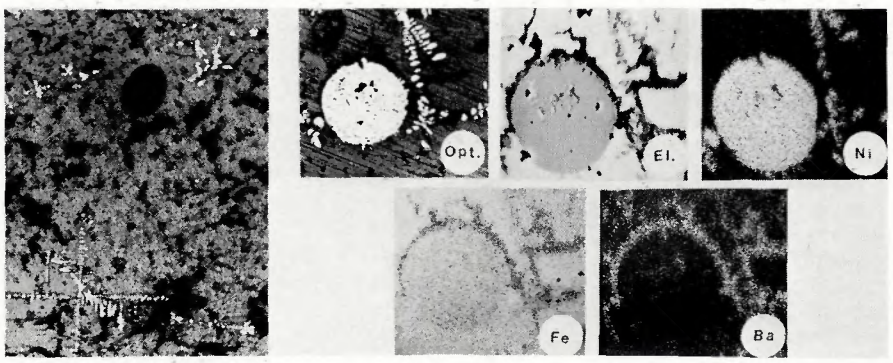

Fig. 6 — Left, typical example of metal dendrites and particles in a $NiO-BaF_2$ slag (X100); right, electron probe analyses of a selected metal dendrite and particle showing high nickel content, absence of nickel in the slag and the lack of miscibility between the FeO reaction product and the inert BaF_2 slag (X600). Photomicrographs reduced 54%

Table 4 — Nickel Transfer from Oxide Slags to Pure Iron

Flux composition wt% NiO	Flux content, wt% Ni	Slag composition, wt% Ni	Ingot composition, wt% Ni Top	Bottom
5 $NiO-BaF_2$	2.9	0.01	4.4	4.8
10 $NiO-BaF_2$	5.6	0.05	15.2	15.6
15 $NiO-BaF_2$	10.8	0.01	13.6	14.0
20 $NiO-BaF_2$	12.4	0.09	16.6	14.8
25 $NiO-BaF_2$	17.2	0.19	34.8	34.8
20 $NiO-MgF_2$	11.8	0.50	4.2	4.6
35 $NiO-MgF_2$	25.6	1.21	22.1	23.7

Table 5 — The Effect of Electrode Feed Rate on Ni Transfer to Fe

Flux	Electrode Feed Rate, m/hr	Slag composition wt% Ni	Ingot composition, wt% Ni
25 $NiO-BaF_2$	114	0.19	34.8
	284	0.50	13.5

Table 6 — Voltage and Current Levels for Varying Aluminum Electrode Feed Rates

Electrode feed rate, m/hr	Voltage, v	Current, amp
114	65	50
183	65	100
284	65	200

Table 7 — Nickel and Copper Transfer to Iron

Flux	Flux composition, wt%	Ingot composition, wt%	Slag composition, wt%
25 NiF_2-BaF_2	12.14 Ni	12.48 Ni	0.91 Ni
20 $NiCl_2-MgF_2$	10.00 Ni	4.13 Ni	8.66 Ni
25 $CuO-BaF_2$	18.34 Cu	24.58 Cu	0.92 Cu

Table 8 — Mn Transfer from MnO_2 Slags to Pure Iron

Flux composition, wt% oxide	Ingot composition, wt% Mn	Slag composition, wt% Mn	wt% Fe
100 MnO_2	0.70	51.2	23.4
20 MnO_2-BaF_2	0.38	9.84	6.60

composition — Fig. 7. But the overall reaction rate was much lower in that only about half of the copper in the slag was transferred to the ingot — Fig. 8.

In the melted areas of the droplet tips, the copper level and microstructure were similar to that of the ingot, showing that the reaction took place virtually entirely at the electrode tip. There was some inhomogeneity in the droplet and evidence for a somewhat higher copper concentration around the neck of the drop, but not on the scale observed with nickel transfer; there was no evidence of a copper-rich surface layer — Fig. 9. This suggests that in this reaction the transfer of the copper reaction product into the droplet is more rapid than its formation at the drop surface.

The slags contained areas which were rich in copper and poor in aluminum, and others that contained some aluminum but virtually no copper. This indicated that the reaction process was subjected to spasmodic interference, presumably related to the evolution of the gaseous aluminum chloride and the accompanying intermittent submerged arcing. The slags also contained metallic droplets which were virtually pure copper, despite the fact that aluminum was being deposited — Fig. 10. Thus small aluminum droplets created in the metal transfer process apparently react completely with the slag to produce pure copper droplets and aluminum chloride, which disperses.

These observations suggested that, at the electrode tip, insufficient time was available to react all of the available copper chloride with aluminum. To determine the effect of reaction time two further experiments were carried out. In the first, the electrode feed rate was altered to change the time available for reaction of the electrode tip; in the second, an attempt to reach an equilibrium state was made by melting a mass of aluminum under a molten slag using an inert tungsten electrode and long reaction times.

The changes in the electrode feed rate were made with the 25 wt% $CuCl_2$ flux to maximize any effect on the copper transfer. The operating current increased with feed rate, but there was no change in the operating voltage — Table 6. Ingot concentrations decreased with increasing feed rate (Fig. 11), showing the extent of reaction to be kinetically determined. In the inert electrode experiments an arc was struck on a 50 gm piece of aluminum under an argon shield and flux was then added until the arc was extinguished and electroslag conditions were achieved. These melts differed from

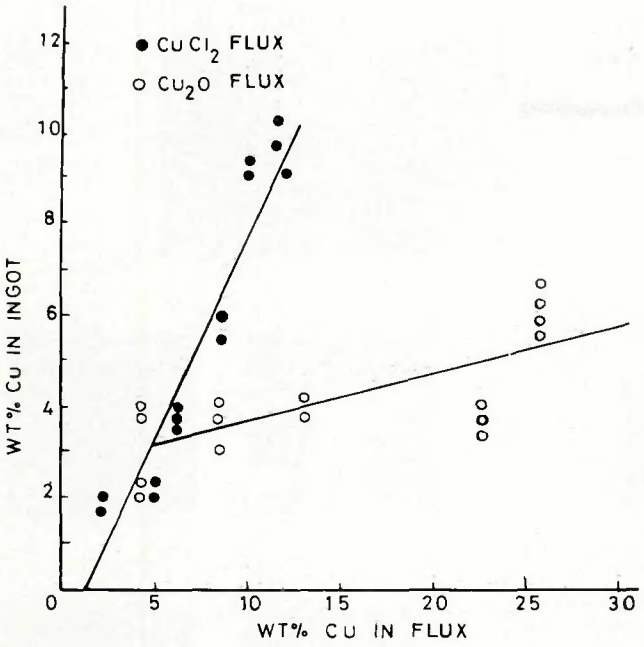

Fig. 7 — Ingot composition vs. flux composition for pure Al melted into $CuCl_2$ containing slags which form a gaseous reaction product and Cu_2O bearing slags which give rise to a solid reaction product

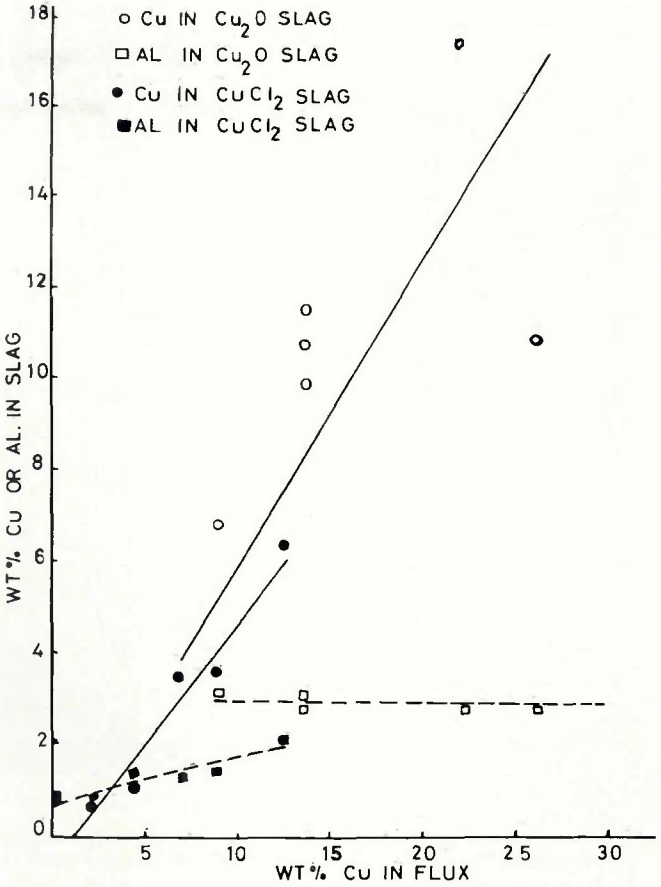

Fig. 8 — Slag composition vs. flux composition for $CuCl_2$ and Cu_2O bearing fluxes

the consumable electrode melts in two ways: first, electrode negative polarity was used, and second, the melting was carried out in the transparent crucibles to avoid excessive heat loss with the water cooled crucibles.

Fluxes containing 5 and 25 wt% $CuCl_2$ were used with an operating current of 100 amp for a 3 min period (longer melting times brought on a collapse of the silica crucibles). A condition close to the reactive limit was reached with the 5 wt% $CuCl_2$ flux, since the slag contained only 0.10 wt% Cu; with the 25 wt% $CuCl_2$ flux most of the copper was again transferred, but there was a higher proportion (1.92 wt%) left in the flux after 3 minutes.

These experiments indicate that the transfer of copper to aluminum occurred at a much lower rate than the transfer of nickel to iron because of the formation of a gaseous reaction product. To ensure that some other factor inherent in the change of systems was not responsible for this result, further experiments were made with transfer to iron in which NiF_2, $NiCl_2$ or CuO was added to the inert flux. The addition of $NiCl_2$ gives rise to a definite gaseous reaction product, the CuO to a liquid product and the NiF_2 addition probably to a liquid close to its boiling point — Table 3. In all cases the reaction is thermodynamically highly favorable. It was found (Table 7) that with the fluoride and oxide additions there was a very high level of transfer of reactant to the ingot, as with NiO in the flux. On the other hand, with the chloride addition the transfer was much reduced as with the transfer of copper to aluminum.

Solid Reaction Product. A high driving force with a solid reaction product was obtained by melting aluminum with Cu_2O in the flux — Fig. 3b. The reaction is of the form:

$$3(Cu_2O) + 2Al = 6 \text{ wt\% } \underline{Cu} + \langle Al_2O_3 \rangle$$

The ingots were deposited at the standard 183 m/hr (120 ipm) electrode feed rate, but currents and voltages were more variable during these melts than with the chloride containing fluxes; slag bath temperatures were slightly higher at 1100 ± 50 C and there was more submerged arcing. The extent of copper pick-up as a function of flux composition was similar to that obtained with the $CuCl_2$ fluxes (e.g., up to 5 wt% copper in the flux). Thereafter it was much reduced and large increases in the copper content of the flux caused virtually no increase in the ingot composition — Fig. 7.

The slag composition showed a corresponding loss of copper and pick-up of aluminum — Fig. 8. Alterations in the electrode feed rate had virtually no effect on the copper level in the ingots — Fig. 11. These ingots were cast in a flux containing 12.7 wt% Cu, which was very nearly the same as the copper content of the chloride flux for which the effect of melting rate was determined. The low overall invariant rate of copper pick-up with the oxide flux shows that the barrier to mass transfer was effective and rapidly formed during melting.

Microscopic examination of melted electrode tips and slags showed a similar situation to that resulting from the $CuCl_2$ fluxes, except that the aluminum oxide reaction product was retained in the slag. Very small metallic droplets in the slag were pure copper surrounded by slag containing aluminum — Fig. 10c; larger droplets often retained some metallic aluminum, where with the chloride flux they would have been entirely copper.

Simplified Industrial Reactions

The experiments in the previous section have been concerned with systems which are capable of transferring relatively large quantities of

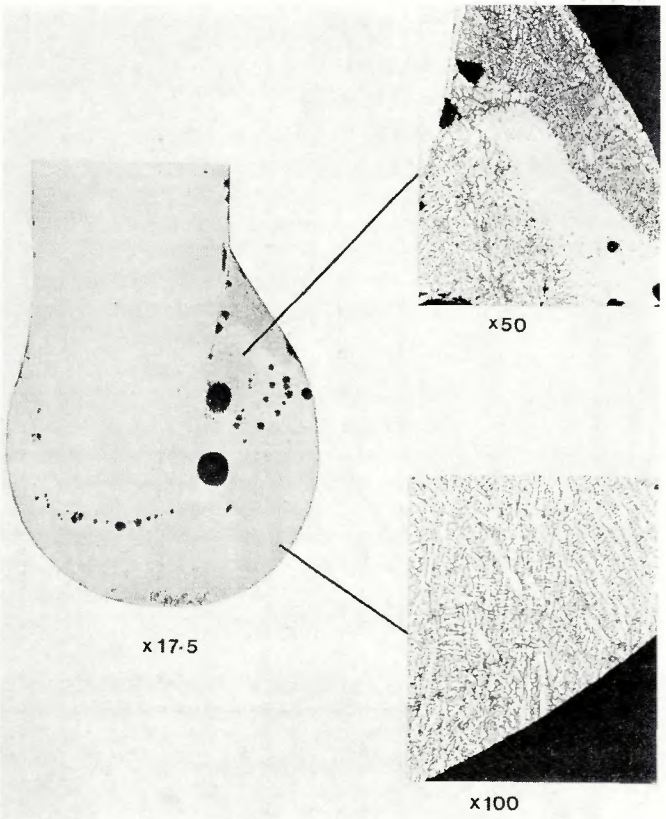

Fig. 9 — Electrode tip from pure Al melted into a $CuCl_2$ bearing flux showing alloying with copper, with a high concentration of copper around the droplet neck, but no copper rich surface layer. The ingot structure was virtually identical with that of the bulk drop structure (reduced 45%)

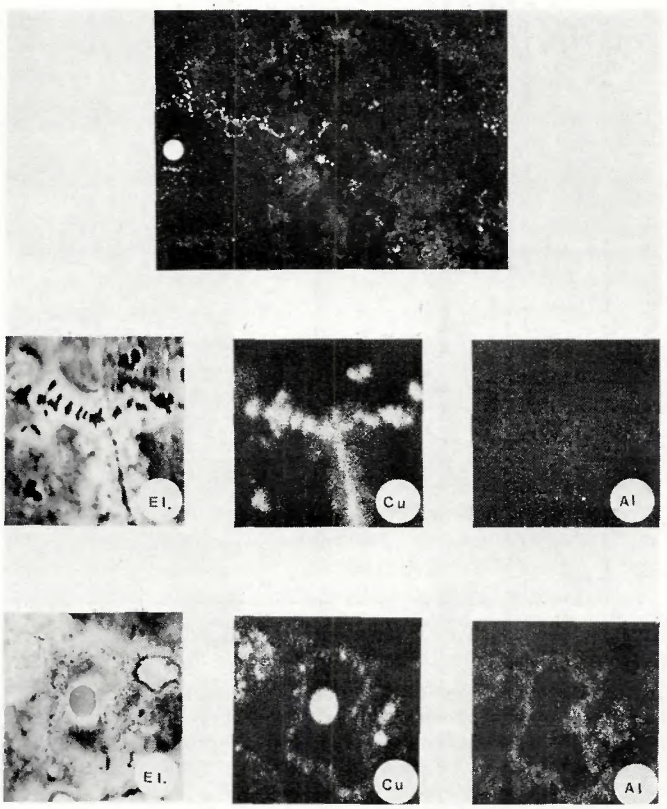

Fig. 10 — Top, metallic droplets formed in $CuCl_2$ and Cu_2O slags (X160); middle row, electron probe analysis of metallic droplets in $CuCl_2$ slags, showing the absence of Al in both metal and slag (X450); bottom row, electron probe analysis of metallic droplets in Cu_2O slags, showing the absence of Al in the droplet, but the presence of Al_2O_3 in the slag (X300). Reduced 45%

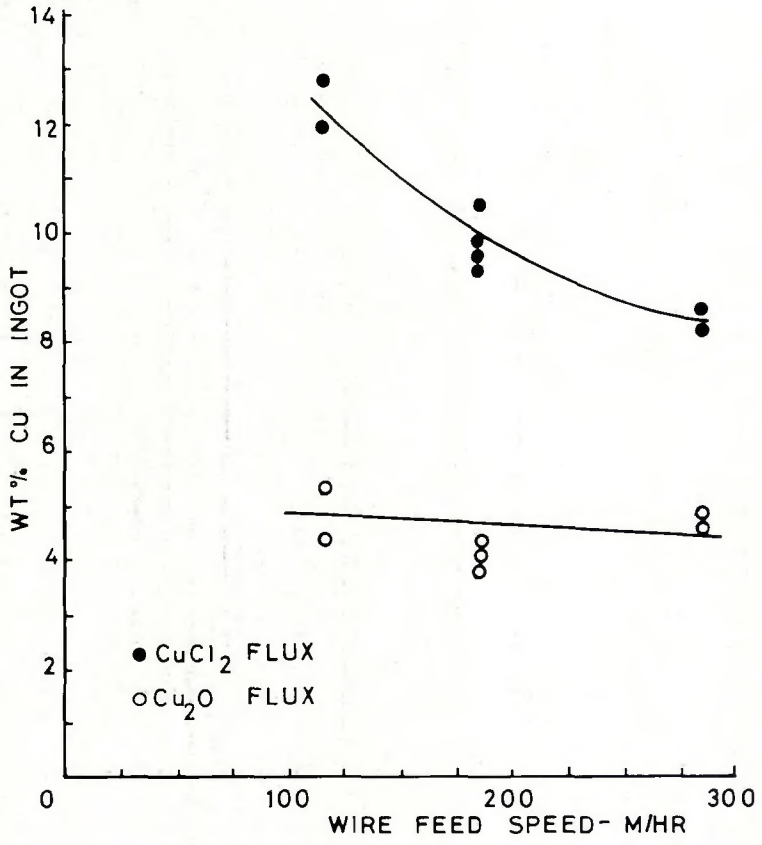

Fig. 11 — Ingot composition vs. electrode feed rate for pure Al melted in $CuCl_2$ and Cu_2O fluxes

elements from the slag to the metal phase because of the high thermodynamic driving force. Results have shown that the extent to which reaction takes place is dependent on the nature of the reaction product, i.e., whether it is liquid, gaseous or solid, and the barrier it therefore creates to further reaction.

Reactions in industrial systems do not involve massive transfer since the primary aim is protection of the weld metal, not extensive oxidation-reduction processes. Also reactions take place not only giving rise to transfer of elements from the slag to the metal, but also from the metal to the slag. In this section much more limited reactions are considered, involving the transfer of elements typically found in industrial systems based on iron and steel, i.e., silicon, manganese, and carbon and the effect of putting various oxides in the flux. In some cases these reactions have been enhanced by going well beyond the concentrations used industrially, so as to make their effects more obvious.

The Transfer of Si from a SiO_2-Containing Flux. In these experiments SiO_2 additions of up to 30

wt% were made to the inert BaF_2 and MgF_2 fluxes, and these were used for melts with pure iron and iron–0.91 wt% silicon electrodes. The potential reaction is the absorption of Si by iron:

$$(SiO_2) + 2_x Fe \rightleftharpoons \% \underline{Si} + 2(Fe_xO)$$

where the reaction product, FeO, entering the slag is liquid and the freed silicon is completely miscible with iron in the liquid state.

With ingots deposited from pure iron electrodes chemical analysis showed that very low levels of silicon transfer took place, since even with 30 wt% SiO_2 in the BaF_2 base the maximum reached was 0.37 wt% Si. Silicon transfer increased rapidly with increase in SiO_2 content of the flux at low levels, but the rate of increase dropped off as the flux SiO_2 content increased — Fig. 12. On a wt% SiO_2 basis the MgF_2 based fluxes again transferred less material to the ingot, but on a volume-percent basis the Si transfer was similar in both cases — Fig. 12. Increasing the electrode feed rate from 114 to 284 m/hr (92 to 186 ipm) with the 30 wt% SiO_2–BaF_2 flux did not produce a measurable change in the resulting Si content of the ingot which was 0.30 wt%, i.e., well within the range for ingots cast under standard conditions. Deposition of an ingot with the iron—0.91 wt% Si using the 30 wt% SiO_2 containing flux showed that the equilibrium Si level of the iron had not been reached. This was because there was still Si transfer from the flux to the metal, the Si increasing from 0.91 to 1.07 wt%, although the rate of Si transfer was appreciably lower at this higher Si level.

The SiO_2 content of the slags dropped markedly, in quantities far too large to be accounted for by transfer to the ingot; for instance, the slag from the 30 wt% SiO_2 flux contained 40% less SiO_2. An acrid vapor evolved during melting and was probably SiF_4 which could account for this drop in slag silica level. Neither melted electrode tips nor droplets trapped in the slag revealed any information about the Si transfer, because the Si levels were too low to be observable metallographically or with the electron probe. The unusual slag structure (Fig. 13b) proved to be a result of the association of the SiO_2 in the slag with the FeO reaction product to form some type of iron silicate which was not completely miscible in the inert fluoride base.

The Absorption of Manganese into Iron. Two fluxes were made to evaluate this reaction. One was 20 wt% MnO_2 in a BaF_2 base; the other was pure MnO_2 which, although of no commercial significance at this concentration, provided data for a theoretical analysis of the reaction process (see II under Appendix). Manganese oxides have similar thermodynamic stability to SiO_2 along with similar melting points and solubility behavior, but they have variable oxidation states; as obtained and added to the flux mixture at low temperature the oxide exists as MnO_2 whereas at high temperature in the slag it exists as MnO. The reaction under consideration is thus:

$$(MnO) + Fe \rightleftharpoons \% \underline{Mn} + (FeO)$$

With iron electrodes deposited under standard conditions the transfer of Mn to the ingot was small (less than 1 wt%), but somewhat higher than the transfer of silicon, (Table 8). Large amounts of iron were picked up by the slags. If the MnO_2 is regarded as decomposing completely to MnO and the excess oxygen oxidizes the iron to FeO which goes into solution in the slag, then 97% of the iron content of the slag is accounted for.

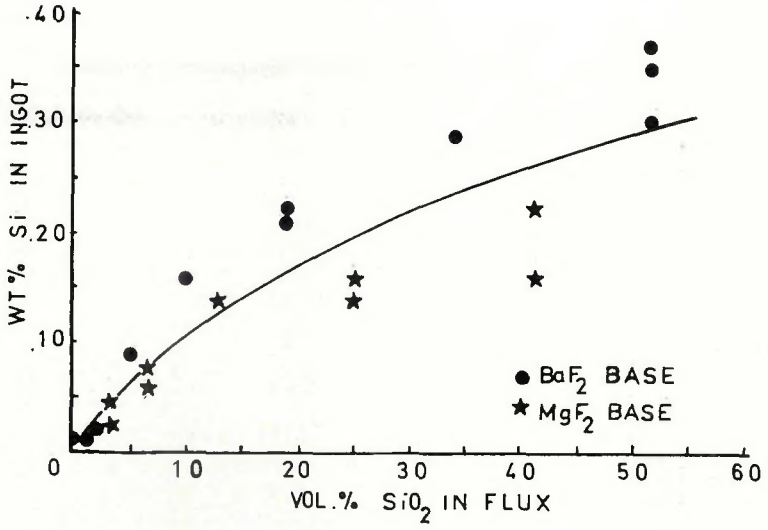

Fig. 12 — Ingot composition vs. flux composition for pure Fe melted in SiO_2 bearing fluxes

Absorption of Elements from Mixed Oxides in the Flux. The effect of having both high and low thermodynamically favorable reactions occurring at the same time was examined by combining NiO and SiO_2 in a BaF_2 base. The fluxes were made up with high and low levels of both reactive compounds combined to make one oxide dominant (fluxes 1 and 2, Table 9) and with the oxides approximately balanced (fluxes 3 and 4). Chemical analysis of the ingots produced under standard conditions showed that Ni transfer occurred at the levels expected, but that very little Si transfer took place with any of the fluxes — Table 9.

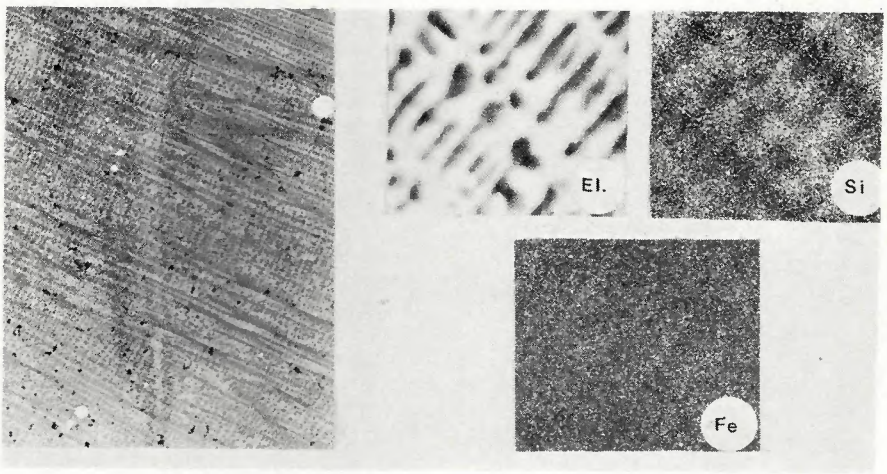

Fig. 13 — The structure of SiO_2 slags: left, the duplex phase structure (X160); right, the electron probe analysis revealing the association of SiO_2 and FeO in the slag (X1000). Reduced 42%

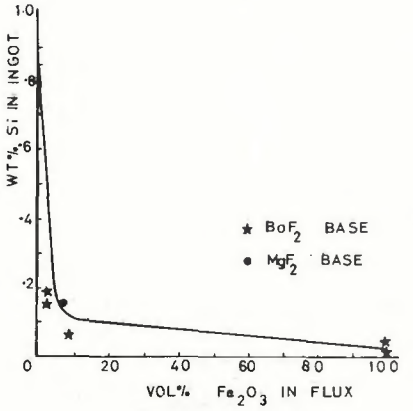

Fig. 14 — Ingot composition vs. flux composition for a 0.91 wt% Si-Fe alloy melted into Fe_2O_3-bearing fluxes

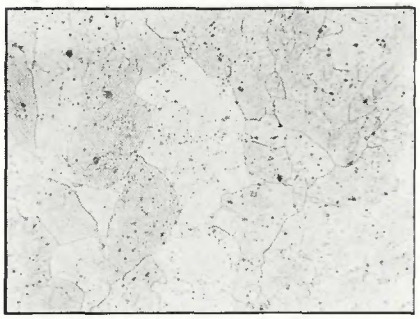

Fig. 15 — Oxide inclusions showing transfer of oxygen into the bulk metal in an ingot produced from 0.91 wt% Si-Fe alloy melted in a pure Fe_2O_3 flux. X100 (reduced 45%)

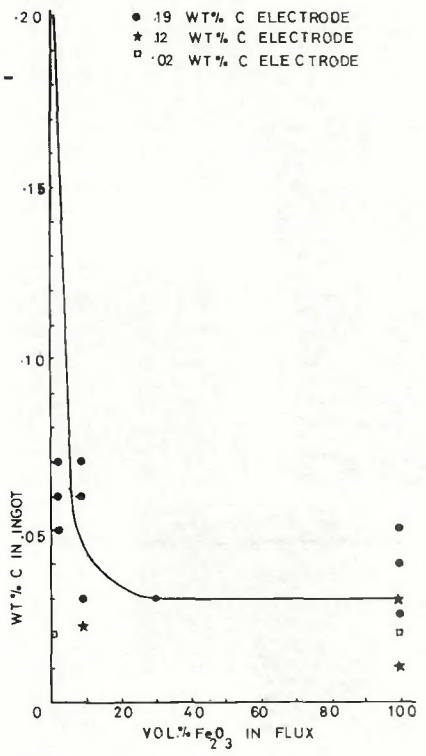

Fig. 16 — Ingot composition vs. flux composition for iron-carbon alloys melted into Fe_2O_3-bearing fluxes

The Loss of Silicon from 0.91 wt% Si-Iron Melted in an Oxidizing Flux. The experimental work up to this point has considered only the transfer of elements from the slag to the metal. An equally important reaction, especially in practical welding situations, is the loss of alloying elements in the metal to reactive slags. A simple reaction of this type was investigated by melting 0.91 wt% Si-Fe alloy in fluxes containing Fe_2O_3, where the reaction is:

$$\% \underline{Si} + 2(Fe_xO) \rightleftarrows 2_xFe + (SiO_2)$$

This reaction has a high thermodynamic driving force and liquid reaction products.

With small amounts of Fe_2O_3 in the flux there was marked loss of Si from the metal which dropped from the original level of 0.91 to 0.1 wt%, Fig. 14. With further increases in Fe_2O_3, even to 100%, there was little further change. This loss of Si from the metal to the slag was much greater than the reverse reaction of absorption from the slag into the metal. Increasing the electrode feed rate to 284 m/hr (186 ipm) had no effect on the residual Si level. There was evidence for considerable excess oxygen in the electrode tips and the ingot structure which appeared as inclusions on solidification — Fig. 15.

Carbon Loss in Iron Oxide Fluxes. Iron-carbon alloys at three levels of carbon content (0.19, 0.12 and 0.02 wt%) were melted into the Fe_2O_3 - containing fluxes. The reaction under consideration is:

$$(Fe_xO) + \% \underline{C} = x\,Fe = [CO]$$

where the reaction product CO is gaseous. There was a large reduction in the carbon level with small additions of oxide to the flux — Fig. 16. This was similar to the silicon loss observed with the iron-silicon alloy. The low carbon (0.02 wt% C-Fe) alloy was, however, apparently unaffected by the melting operation. The effect of an increased electrode feed rate was investigated with the 0.19 wt% C-Fe alloy and two fluxes — pure Fe_2O_3 flux and the 5 vol % Fe_2O_3-BaF_2 flux. The increase in electrode feed rate caused some loss of control over the voltage and current with voltages fluctuating between 10 and 40 v and the current between 500 and 1000 amp. However, there was no apparent change in the carbon content of the ingots within the range of experimental scatter observed with the standard feed rate of 114 m/hr (92 ipm) — Table 10.

The electrode tips of iron-carbon alloys melted into the pure oxide flux rarely contained any melted material. However, in the oxide-fluoride flux experiments the electrode tips retained some melted material and provided more detailed information on the progress of the reaction. Figure 17 shows three important features of the carbon oxidation process:

1. The slag-metal interface is very irregular.
2. Porosity is present at the solid metal-liquid metal interface.
3. The melted metal is apparently devoid of carbon and full of oxide inclusions.

These facts show that decarburization was taking place throughout the molten metal and that the resultant gas evolution fragmented the electrode tip continuously during melting. The ingot carbon level in this particular case was 0.023 wt%, cast from a 0.12 wt% C electrode. In approximate terms, the loss of 0.10 wt% C to form CO at 1900 C produced 120 cm^3 of gas for each cm^3 of iron, to cause the porosity and fragmentation observed. The oxide inclusions are the result of the increase in oxygen level, which rose from 0.0015 wt% in the 0.12 wt% C iron to 0.0187 wt% in the ingot.

In the slags a larger amount than usual of iron particles was found due to the explosive nature of the transfer process. The evolution of CO gas continued in small metal droplets in the slag, although there was little evidence of carbon remaining in the metal — Fig. 18. This is consistent with the observations in the copper chloride-aluminum experiments where the reaction continued in small metal droplets suspended in the slag until all of the aluminum was consumed and copper remained.

Carbon Loss with Fluxes Containing Various Oxides. Further experiments on the oxidation of carbon were made with the 0.19 wt% C-Fe alloy using a series of fluxes which contained oxide additives varying in reactivity from CuO to the most stable available oxide, CaO. In some cases the fluxes would not support the standard voltage and current (50–60 v, 400–450 amp) at the 114 m/hr (92 ipm) feed rate; the electrode feed rate was then maintained and the electrical power values allowed to adjust to the slag characteristics.

It is apparent that the degree of carbon oxidation is related to the thermodynamic stability of the oxide and, correspondingly, so is the amount of alloy element transferred to the ingot — Table 11. With any oxide in the flux there was some loss of carbon; only by melting in pure fluoride was all the carbon retained. It must be pointed out, however, that this carbon loss would not occur with commercial fluxes which are fused in graphite crucibles and there-

by pick up carbon which transfers to the deposited metal; the fluxes used in the present work were made by solid state sintering, specifically to avoid contamination by crucible materials.

Discussion

The results of the present work show that in electroslag melting it is possible, with an inert flux and inert gas coverage, to deposit metal of the same composition as the electrode. Alternatively, it is possible to some extent to control the composition of the melt by adjusting the composition of the flux. These attributes of the electroslag system are not readily attainable with arc welding, because arc welding cannot be carried out with inert fluxes or with fluxes designed simply to obtain compositional control of the weld metal. Arc welding fluxes require constituents that promote arc stability, adequate penetration, ease of slag removal, etc.; they do not therefore have the flexibility of electroslag fluxes. The authors tried to investigate slag-metal reactions in arc welding with a range of flux compositions in a similar way to the present investigation. In the vast majority of cases, however, no control of the system was possible due to arc instability.

The Processes of Reaction

The reactions that take place in electroslag welding do so primarily at the electrode tip. There are two reasons for this — the high surface-to-volume ratio and the rapid transport processes. Spherical droplets of 1 to 4 mm diam (which embraces the observed range of droplet sizes) have surface-to-volume ratios of 15 to 60, whereas 50 to 100 gm ingots of 2.5 mm diam have ratios between 0.35 and 0.7. There is thus an overwhelming increase in surface area for a given volume at the electrode tip.

Current enters the slag through the constricted area of the electrode tip and then broadens out to take the path of least resistance. It was shown by Maecker,[14] and the concept applied to welding systems by other workers, [12,15] that where a current path through a fluid broadens out for a constriction there occurs a Lorentz force-induced high velocity motion of the fluid away from the constriction. Applying Maecker's formula for the maximum velocity of flow gives a value of about 50 cm/sec for the NaF-KCl slag used with the aluminum melts (see I under Appendix), compared with the experimentally measured value of 50-65 cm/sec. Higher theoretical values are obtained for the steel slags —

Table 9 — Ni and Si Transfer from Combined Driving Force Fluxes

Flux No.	NiO, wt%	SiO_2, wt%	BaF_2, wt%	Ingot composition, wt% Ni	wt% Si
1	25	2.0	73	22.5	0.02
2	5	20	75	4.7	0.01
3	25	15	60	22.0	0.06
4	5	2.5	92.5	3.9	0.02

Table 10 — Carbon Oxidation at Increased Electrode Feed Rates

Flux	Electrode feed rate, m/hr	Voltage, v	Current, amp	Ingot composition, wt% C
Fe_2O_3	114	30	400	.026–.050
	229	15	1000	.02
5 vol% Fe_2O_3–BaF_2	114	50	400	.03 –.07
	183	30	600	.02 –.05
	284	20	800	.02 –.04

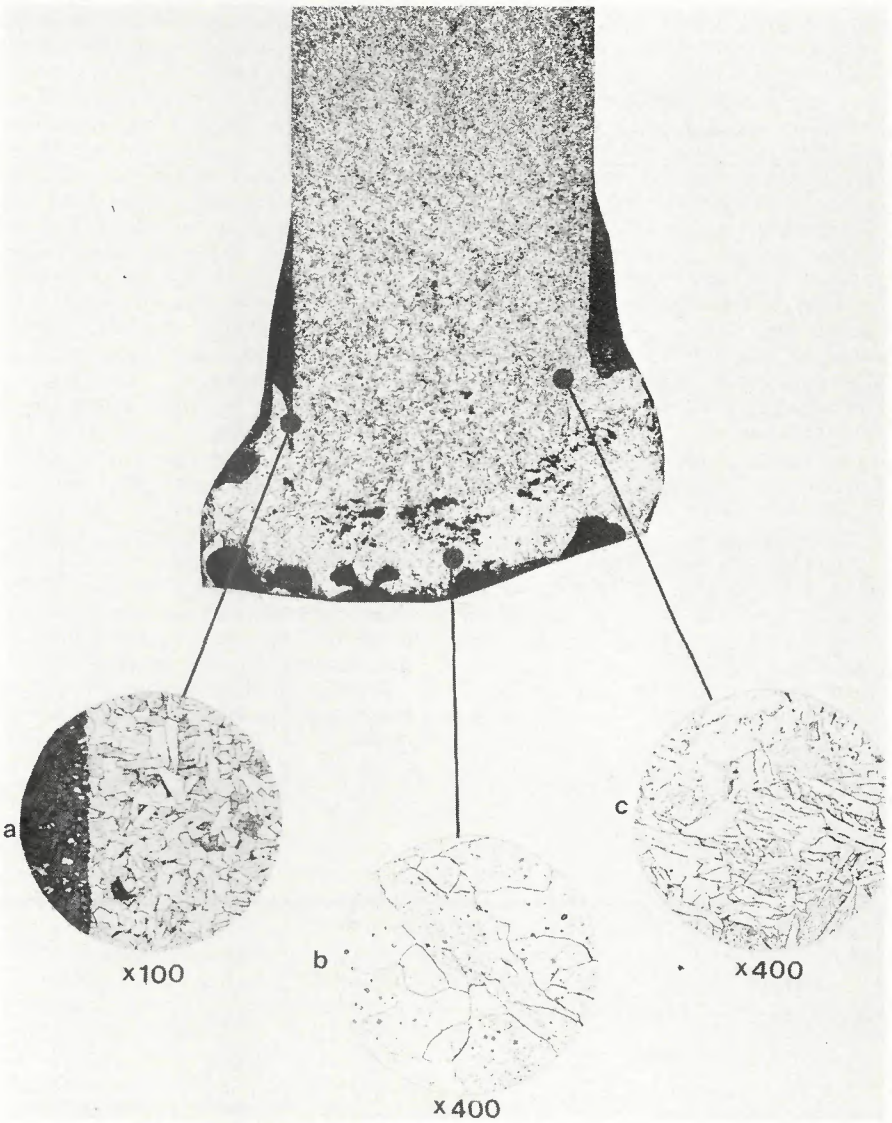

Fig. 17 — The melted electrode tip of a 0.12 wt% C-Fe alloy melted in an 8 vol-% Fe_2O_3-BaF_2 flux, showing the explosive effect of CO evolution at the slag-metal and liquid metal-solid metal interfaces (X 20). The details show (a) metal droplets expelled at the start of oxidation; (b) oxide inclusions and the absence of carbon in the oxidized molten metal; and (c) the iron-carbon transformation microstructure near the liquid metal-solid metal interface. Reduced 32%

115 cm/sec for MgF_2 and 90 cm/sec for BaF_2. There is thus rapid transport of reacting constituents in the slag.

Similarly, although it is not possible to estimate its magnitude, there will be fluid motion within the molten droplet due to the broadening out of the current path from where it enters the slag through the constricted area of the solid electrode at the slag surface. At the ingot, current will enter the surface at something approaching uniform current density. Taking aluminum melts made at 150 amp this would give a current density of 30 amps/cm^2, compared with 2,000 amp/cm^2 at the electrode. This low current density cannot give rise to any significant degree of motion so that there will be only comparatively slow transport of constituents in the ingot.

A similar intense reaction at the electrode tip occurs between the gas phase and the molten metal in arc welding, although the reaction temperature is considerably higher. But whereas there is also considerable reaction with the deposited metal in arc welding, there is much less reaction in the electroslag system. This is because, in arc welding, there is firstly a high reaction temperature where the arc impinges on the surface of the weld pool; second, there are rapid, Lorentz force-induced, transport processes within the weld pool; and, third, there is a high degree of super-heat of the molten metal.

All of these are absent in electroslag deposition. Thus electroslag welds tend to be much more free from compositional and associated defects than are arc welds. Where reactions do occur, however, they do so relatively rapidly so that in the electroslag system any reacting constituents in the flux are soon used up and are only replaced on 'topping up'. With arc welding, on the other hand, there is a continuous supply of fresh flux. From this point of view the chemical composition of electroslag deposited metal is, therefore, less under control.

Reaction at the Electrode Tip. The active constituent in the slag is swept, by the Lorentz force-induced motion, towards the reacting surface of the molten electrode tip. Within the metal drop the Lorentz force is also acting to produce fluid motion that distributes the reaction product throughout the bulk of the drop. The evidence from the present work, together with established knowledge of the type of motion produced by the Lorentz force, suggests that at the slag-metal interface the two motions will oppose each other as in Fig. 19. As the slag approaches close to the interface, the velocity goes through a transition from that in the bulk of the slag to that of the interface. The slag and metal at the interface thus move together (or would be stationary if the two motions exactly balanced). The slag motion does not, therefore, carry the reacting constituent right up to the interface.

At the interface itself the reaction denudes the slag of reacting material, and the supply of further reactant is then determined by diffusion through the boundary layer from the high concentration in the rapidly replenished bulk of the slag. The reacting constituent in the metal is likewise transported towards the interface by the bulk, Lorentz force-induced motion and then has to pass, by diffusion, through a boundary layer to arrive at the interface. The products of reaction are dispersed by the reverse processes of diffusion away from the reaction interface through the boundary layers into the high velocity regions where there is rapid dispersal into the bulk material. It is the rate of diffusion of reactants to the interface, or of reaction products away from it, that determines the rate of reaction.

A convenient system to analyze in more detail is that of the transfer of nickel, from NiO containing fluxes, into iron. Clearly the rate of transfer is high so that the flux is virtually completely denuded of nickel — Table 4. However, with 25 wt% NiO in the flux solidified droplets show that a high level of Ni transfer was still taking place at the end of the melt despite a low concentration in the flux. The droplet in Fig. 5a shows the existence of a nickel rich surface boundary layer of about 2 x 10^{-3} cm thickness. This is consistent with a high velocity slag motion that gives rise to a thin boundary layer on the slag side of the reaction interface, and a lower degree of fluid motion within the metal droplet, and therefore a thicker boundary layer on the metal side of the interface. Diffusion across the metal boundary layer then becomes the rate controlling process.

Since the transfer of Ni into Fe is a thermodynamically highly favorable reaction there will be a virtually 100% concentration of nickel at the metal surface (see II under Appendix). There is then a high concentration gradient in the metal boundary layer causing diffusion of nickel into the bulk of the droplet where it is taken up by bulk transport processes and distributed comparatively uniformly throughout the drop. A calculation of the concentration of Ni built up in the drop, due to diffusion through the boundary layer during the period of growth of the droplet on the end of the electrode, gives a result of 10 to 20 wt% nickel (see Appendix III) the range being primarily due to the difficulty in assigning values to the diffusion coefficient. This compares with the experimentally determined concentration of nickel in the droplet of about 15 wt%.

In addition to the diffusion of nickel through the periphery of the drop there is also an important contribution from the reaction taking place by a similar diffusion process through the layer of molten metal formed on the tapering electrode above the drop — Fig. 19. Here there is a very high surface area-to-volume ratio and thus a very high concentration of nickel as shown by analyses

Table 11 — Carbon Oxidation by Oxide Fluxes

Flux composition, wt% oxide	Operating conditions, v	amp	Ingot composition, wt% C	wt% X
25 CuO-BaF_2	45	300	.031	29.3 Cu
25 NiO-BaF_2	55	400	.02	35.8 Ni
25 Cr_2O_3-MgF_2	60	250	.024	2.59 Cr
25 MnO_2-BaF_2	50	400	.05	0.46 Mn
35 SiO_2-BaF_2	50	400	.07	0.70 Si
30 TiO_2-BaF_2	60	200	.12	0.01 Ti
20 MgO-MgF_2	55	350	.13-.16	—
30 Al_2O_3-BaF_2	70	200	.13	0.02 Al
50 BaO-MgF_2	25	400	.12	—
25 CaO-BaF_2	65	400	.16	—
BaF_2	55	400	.19	—

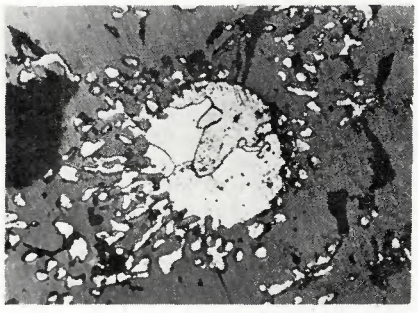

Fig. 18 — Fe-C droplet disintegrating in an iron oxide slag due to CO evolution. X400 (reduced 45%)

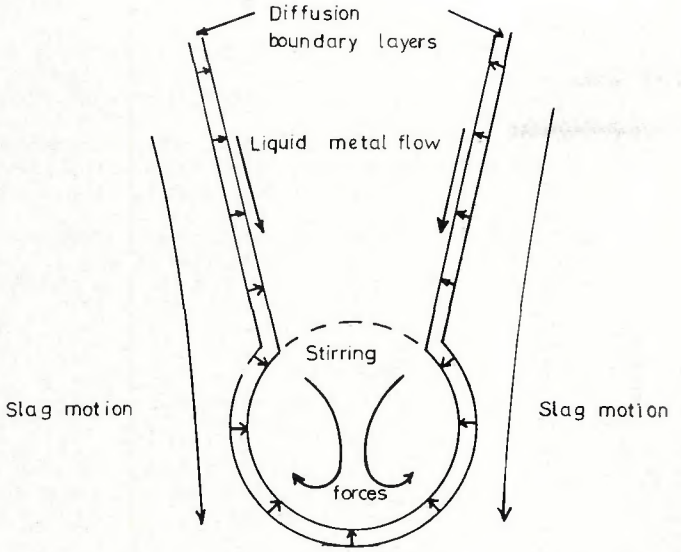

Fig. 19 — Schematic diagram of the physical conditions at the electrode tip during slag-metal reactions

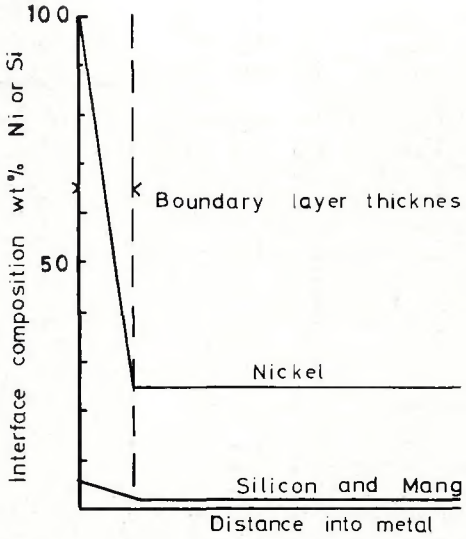

Fig. 20 — The effect of the thermodynamic driving force on the concentration gradient in the metal phase boundary layer for slag-to-metal transfer

of the material around the neck of the drop of around 60 wt% Ni. All the molten metal is transferred across into the ingot where it mixes to give a mean composition of around 22–24 wt%. At lower levels of NiO in the flux the same processes of nickel transfer will be rate controlling until the concentration of Ni in the slag is so reduced that the rate of diffusion across the slag boundary layer is less than the rate of diffusion across the metal boundary layer.

The mechanism of transfer of manganese and silicon from the slag into the iron should be the same as the transfer of nickel, with the same boundary layer characteristics, except that the concentration gradient is much lower. A driving force provided by a concentration of 100% nickel at the slag-metal interface resulted in a concentration of nickel in the ingot of about 25% of this level. Thermodynamic calculations (see II under Appendix) show that for a slag of pure manganese oxide the equilibrium concentration of manganese at the metal surface would be about 2.2 wt%; there is thus a much lower driving force (Fig. 20), but the ingot composition was about the same proportion of the concentration at the metal surface, i.e., 30%, or 0.7 wt%. For the flux containing 20 wt% manganese oxide the ratio of manganese in the ingot to that at the metal surface works out at about 27%.

The data for silicon are more difficult to interpret since the silica and iron oxide form a complex silicate — Fig. 13. This makes it difficult to assign values to the crucial parameters of activity of the silicon and iron in the slag. However, the experimentally observed silicon levels in the ingot would again appear to be compatible with a ratio of about 25% of the equilibrium silicon level at the metal surface.

Where a gaseous reaction product is formed, as with the reaction between $NiCl_2$ in the flux and iron, or with the absorption of copper into aluminum from a slag containing $CuCl_2$, the bubbles forming at the interface interfere with the diffusion of reactant through the slag boundary layer. A typical aluminum ingot would absorb 5 wt% copper. For a drop of 1 gm with a diameter of 0.35 cm forming on the end of the electrode this would give rise to the evolution of 55 cm^3 of aluminum chloride gas, forming bubbles and dispersing at the interface during the period of existence of the droplet.

In applying the analysis of diffusion across a boundary layer (see III under Appendix) to diffusion across the slag layer, very approximate calculations, limited because of inadequate knowledge of diffusion coefficients, suggest an "effective thickness" of the slag boundary layer two to three times that of the metal boundary layer. Thus for these systems diffusion through the slag boundary layer becomes rate controlling and there is no evidence of a copper rich boundary layer in the metallographs of the aluminum drop in Fig. 9.

Another feature of the aluminum system is that melting takes place almost perpendicular to the electrode, i.e., the electrode does not become tapered. There is thus little active molten layer on the melting electrode where intense reaction occurs and only a small amount of high copper concentration material at the neck of the drop so that the copper concentrations of the droplet and the ingot are almost the same.

The reduction of carbon in iron by oxides in the flux, involving as it does a gaseous reaction product, invites comparison with the $CuCl_2$–Al system. But there is an essential difference between the two cases. With the Al-$CuCl_2$ system the gaseous reaction product is formed at the slag-metal interface. In the FeO-C system on the other hand, oxygen is first absorbed into the iron and this circulates and comes into contact with the carbon within the body of the drop giving rise to gas formation and fragmentation of the drop. This further increases the surface area and the rate of reaction, so that the carbon is rapidly removed. Only comparatively small quantities of FeO in the slag are required to remove most of the carbon because of the high activity of FeO at low concentrations in fluoride slags.[16]

The removal of silicon from iron with slags containing FeO occurred to a much greater extent that the reverse process of absorption of silicon from the slag. This is because the situation is similar to the removal of carbon in that oxygen is taken into the body of the metal droplet and oxidation of silicon occurs throughout the bulk of the droplet as well as at the slag metal interface. The effectiveness of small amounts of FeO in silicon removal is again due to the enhanced activity of low concentrations of FeO in fluoride slags.

When an insoluble reaction product is formed, as with the Cu_2O-Al system, some of the reaction interface is blocked off. This limits the rate of reaction. The marginal in-

crease in the ingot Cu levels with large increases in Cu content of the slags indicates that a relatively constant reduction of area is achieved and that the reaction proceeds only if the oxide film is then removed or disturbed. Such a disruption will occur every time a droplet is removed from the electrode tip; it will probably also occur when irregularities caused by submerged arcing, itself brought about by the presence of the oxide film, take place.

Conclusions

1. Slag-metal reactions take place primarily at the molten electrode tip due to the high surface-to-volume ratio of the molten metal and the intense stirring forces. Reactions continue in small droplets contained in the slag and created by the metal transfer process. Reactions at the ingot surface are limited because of the low surface-to-volume ratio and much weaker stirring forces.

2. Slag motion is caused by the Lorentz force as a result of the drop in current density between the electrode and the conductive slag bath, and the Lorentz force also causes circulative mixing within the liquid metal formed on the electrode tip. These stirring forces act to distribute reaction products from the slag-metal interface into the bulk of the slag and metal phases.

3. The Lorentz force induced motion carries the reactants in the slag and in the metal towards the slag-metal interface. At the interface itself the motion is the same for both slag and metal, so that the final transport to the interface is by diffusion through boundary layers in the slag and metal. For most reactions diffusion across the metal boundary layer is rate controlling.

4. The concentration, or activity, gradient determining the extent of diffusion across the boundary layer is a function of the thermodynamics of the reaction. For a thermodynamically highly favorable reaction there is a high concentration of the reaction product at the boundary layer and hence a high rate of diffusion. Conversely, a low equilibrium level at the boundary layer gives rise to a low concentration gradient and a low rate of transfer.

5. The rate of reaction is reduced when the reaction product formed at the interface is gaseous because it interferes with the transport of material to the interface and, when a solid reaction product is formed, it blocks off areas of the interface from reaction. The rate of reaction is particularly high where the reactant in the slag is soluble in the metal, and it is transported into, and reacts with elements in, the bulk of the metal. This occurs with the oxidation by FeO in the slag of silicon and carbon in iron, whereby oxygen enters the iron and reacts with the silicon and carbon throughout the molten droplet.

6. Complete equilibrium is not achieved in slag-metal reactions. For reactions occurring at the interface under the conditions investigated in the present work, about 30% of the equilibrium level concentration of reaction product was attained in the deposited metal provided there was no prior depletion of the supply of reactant from the slag. For reactions occurring throughout the bulk of the molten droplets equilibrium was much more closely approached.

Acknowledgements

The authors wish to thank Professor E.C. Rollason, Head of the Department of Industrial Metallurgy at the University of Birmingham, for his interest and encouragement, and the Ministry of Defence (Navy Dept.) for financial sponsorship of this project. We also wish to thank Dr. P. J. Emerson and Mr. M. Burke of B.C.I.R.A. for their generous assistance on the electron microprobe work.

References

1. Fitch, I. C., "Whither Electrode Design?", *British Welding Journal,* 7 (10), 600 to 604, 1960.

2. Babcock, D. E., "The Fundamental Nature of Welding, Part V — The Physical Chemistry of the Arc-Welding Process," *Welding Journal,* 20 (4), Research Suppl., 189-s to 197-s, 1941.

3. Bennett, A. P., and Stanley, P. J., "Fluxes for submerged-arc welding of Q.T.35 steel," *British Welding Journal,* 13 (2), 59 to 66, 1966.

4. Belton, G. R., Moore, T. J., and Tankins, E. S., "Slag-Metal Reactions in Submerged Arc Welding," *Welding Journal,* 42 (7), Research Suppl., 289-s to 297-s, 1963.

5. Claussen, G. E., "The Metallurgy of the Covered Electrode Weld," Ibid., 28 (1), 12 to 24, 1949.

6. Chipman, J., and Christensen, N., "Slag-Metal Interaction in Arc Welding," Welding Research Council Bulletin No. 15, 1953.

7. Bagryanskii, K. V., and Lavrik, P. F., *Welding Production,* 11 (5), p. 72, 1964.

8. Baryshnikov, A. P., and Petrov, G. L., *Welding Production,* 15 (10), p. 9, 1968.

9. Hazlett, T. H., "Coating Ingredients Influence on Surface Tension, Arc Stability and Bead Shape," *Welding Journal,* 36 (1), Research Suppl., 18-s to 22-s, 1957.

10. Duckworth, W. E., and Hoyle, G., *Electroslag Refining,* Chap. 3, Chapman & Hall, London, 1969.

11. Crimes, P. B., "Rates of Mass Transfer in Electro-slag Remelting—Part 1: Model Studies," BISRA Report Mg/A/72/64, 1964.

12. Woods, R. A., and Milner, D. R., "Motion in the Weld Pool in Arc Welding," *Welding Journal,* 50 (4), Research Suppl., 163-s to 173-s, 1972.

13. Paton, B. E., *Electroslag Welding,* Chap. 3, AWS, 1962.

14. Maecker, H., *Z. Physik,* vo. 141, p, 198, 1955.

15. Salter, G. R., and Milner, D. R., "Gas Absorption from Arc Atmospheres," *British Welding Journal,* 7 (2), 89 to 100, 1960.

16. Davies, M. W., "The Chemistry of CaF_2-based Slags," International Symposium of Metallurgical Chemistry, Sheffield, 1971.

17. *Basic Open Hearth Steelmaking,* 3rd Ed., Chap. 16, AIME, 1964.

18. Edwards, J. B., et al, *Metals and Materials,* 2 (1), p. 1, 1968.

Appendix

I. Slag Velocity Near the Electrode Tip

The velocity of flow in a plasma jet created by a constriction in the current path is:[13]

$$V_{max} = \sqrt{\frac{2I^2}{\rho \pi a^2}}$$

where I = absolute amperes, ρ = fluid density, and a = radius of constriction.

In this case, the current is 150 amp (15 amp absolute), the fluid density is that of the NaF-KCl eutectic (approx. 2 gm/cc), and the radius of the constriction is the radius of the electrode (1.6 mm). Thus:

$$V_{max} = \sqrt{\frac{2(15)(15)}{2\pi(0.16)^2}} = 53 \text{ cm/sec}$$

In the MgF_2 and BaF_2 slags, the current is 400 amp (40 amp absolute) and the densities approximately 3 gm/cc and 4.5 gm/cc respectively. This gives velocities of 115 cm/sec in MgF_2 and 90 cm/sec in BaF_2.

II. Calculations of the Equilibrium State at the Slag-Metal Interface

A number of the reactions which were investigated with iron electrodes are evaluated thermodynamically to illustrate the principles involved. The temperature at the reaction interface is assumed to approximate to the slag temperature, i.e., 1900 C and thermodynamic data[17] have been extrapolated from steelmaking temperatures to this temperature.

Pure Fe reaction with NiO slags. This is an example of a high rate of reaction with liquid reaction products. Nickel is transferred to the iron according to:

$$(NiO) + Fe \rightleftharpoons \underline{\%Ni} + (FeO)$$

To obtain the free energy of formation:

$$(NiO) \rightleftharpoons \underline{\%Ni} + \underline{\%O};$$
$$\Delta G = +27{,}350 - 35.72T$$

$$Fe + \%O \rightleftharpoons (FeO);$$
$$\Delta G = +28{,}914 - 12.51T$$

Adding

$$(NiO) + Fe \leftrightharpoons \underline{\%Ni} + (FeO);$$
$$\Delta G = +56{,}264 - 48.23T$$

For the equilibrium constant K:

$$\log K = \frac{-\Delta G}{4.575T} = \frac{-12{,}300}{T} + 10.55$$

$$T = 1900\ C = 2173\ K$$

$$\log K = 10.55 - 5.67 = 4.88$$

$$K = 7.6 \times 10^4 = \frac{\underline{\%Ni}\ (a_{FeO})}{(a_{Fe})\ (a_{NiO})}$$

a_{Fe} can be considered as approximately equal to 1. Therefore:

$$\underline{\%\ Ni} = 7.5 \times 10^4\ \frac{a_{NiO}}{a_{FeO}}$$

a_{FeO} cannot be greater than 1, so that even for small values of a_{NiO} the surface layer of the metal will be pure Ni until a_{NiO} becomes too low for the rate of diffusion through the boundary layer in the flux to sustain equilibrium.

Pure Fe Reaction with MnO_x Slags. This is an example of a low rate of reaction with liquid reaction products. At elevated temperatures the reaction is:

$$(MnO) + Fe \leftrightharpoons \underline{\%Mn} + (FeO);$$
$$\Delta G = +29{,}500 - 13.47T$$

At 1900 C and with $a_{Fe} \simeq 1$, this gives

$$K = 1.0 = \frac{a_{MnO}}{a_{FeO}(\underline{\%Mn})}$$

$$\text{i.e.,}\quad \%Mn = \frac{a_{FeO}}{a_{MnO}}$$

A slag containing only manganese and iron oxides is known to behave ideally, so that the activity of each oxide is equal to its mol. fraction. The experiment with pure MnO_2 flux gave a slag containing 51.2 wt% Mn and 21.4 wt% Fe, if 2 wt% Fe is allowed for metal droplets in the slag. Calculations based on these figures give an equilibrium $\underline{\%Mn}$ at the metal surface of 2.2 wt%. If the mutual behavior of the oxides is assumed to remain ideal in the BaF_2 flux, then the 20 wt% MnO – $8aF_2$ flux gives an equilibrium $\underline{\%Mn}$ = 1.6 wt%.

Pure Fe Reaction with SiO_2 Slags. For this reaction:

$$(SiO_2) + 2Fe \leftrightharpoons \underline{\%Si} + 2(FeO);$$
$$\Delta G = +81{,}500 - 28.5T$$

At 1900 C:

$$K = 1.1 \times 10^{-2} = \frac{\underline{\%Si} \cdot (a_{FeO})^2}{a_{SiO_2}\ (a_{Fe})^2}$$

$$a_{Fe} \simeq 1$$

$$\text{so that } \underline{\%Si} = 1.1 \times 10^{-2} \cdot \frac{a_{SiO_2}}{(a_{FeO})^2}$$

The difficulty here is that a_{SiO_2} and a_{FeO} are known not to behave ideally, but the values of a_{SiO_2} and a_{FeO} are not known.

It is clear from the value of the constant that the concentration of Si at the metal surface will be more akin to that of Mn than Ni. The experimental fact that Si was absorbed into iron already containing 0.9 wt% Si, but at a comparatively slow rate, suggests an equilibrium Si level of around 1.5 - 2 wt%.

Fe-C Reaction with FeO Slags. This reaction occurs throughout the bulk of the molten drop which has a temperature of the order of 1600 – 1700 C, say 1650 C. The reaction is:

$$(FeO) + \underline{\%C} \leftrightharpoons Fe + [CO];$$
$$\Delta G = +23{,}600 - 22.0T$$
At = 1650 C:

$$K = 1.35 \times 10^2 = \frac{(a_{Fe})\ (P_{CO})}{(a_{FeO})\ (\underline{\%C})}$$

For virtually pure Fe and pure FeO, $a_{Fe} = a_{FeO} = 1$ and for CO evolved at 1 atm pressure $P_{CO} = 1$.

$$\underline{\%C} = \frac{1}{K} = 0.007$$

This is substantially lower than the experimentally determined range of 0.01 - 0.05% C.

III. Kinetic Considerations

The final concentration, C_f, of nickel in a drop as a result of diffusion through a boundary layer of thickness d in the metal surface is

$$C_f = \frac{Q}{V}$$

where Q is the amount of nickel that has diffused into the drop and V is the final volume of the drop. Q is given by integrating the diffusion through the surface boundary layer of the drop over the period of its development on the end of the electrode:

$$Q = \int_o^t \frac{-DA\ (C_o - C_i)}{d}\ dt$$

where the surface area is a function of time given by:

$$A = (4\pi)^{1/3}\ (3R)^{2/3}\ t^{2/3}$$

where R is the rate of melting of the electrode.

C_o is the concentration at the surface, taken as the equilibrium concentration. C_i is the concentration within the drop — this is taken as constant as the calculation shows it to vary from 0 to about 0.1 C_o. Thus:

$$Q = \left(\frac{D\ (C_o - C_i)\ \ (4\pi)^{1/3}(3R)^{2/3}}{d}\right) \int_o^t t^{2/3} dt$$

Integrating and substituting the final drop diameter, r, for the time of drop formation, t, according to

$$t = \frac{4\pi r^3}{3R}$$

$$C_f = \frac{7.55\ Dr^2}{Rd}\ (C_o - C_i) \quad \cdots\ (3.1)$$

For the transfer of nickel into iron considered in the Discussion R = 0.254 cc/sec, d = 210^{-3} cms., r^2 = 0.063 cm^2, $(C_o - C_i) \simeq C_o$ = 100 wt%. The difficulty is to assign a value to D. From data provided by Edwards[18] D is probably 1 to 210^{-4} cm^2/sec. From this:

C_f = 9.5 for D = 1.10^{-4}
to 19 for D = 2.10^{-4}

List of Symbols

( ) liquid component in slag phase
[ ] gaseous component in slag phase
$\underline{\%\ X}$ alloy component in metal phase
< > solid component in slag phase

Conversion Factors

$C = \frac{5}{9}$ (F – 32)
giving 1100 C $\simeq$ 2010 F
and 1900 C $\simeq$ 3450 F
0 C = 273 K
1 m/hr = 0.66 ipm
1 cm/sec = 23.6 ipm
1 cm^2/sec = 3.9 ft^2/hr
1 cm = 0.395 in.
1 cm^2 = 0.156 $in.^2$
1 cm^3 = 0.062 $in.^3$
1 gm/cm^3 = 3.6 x 10^{-2} $lb/in.^3$